ResearchGate

See discussions, stats, and author profiles for this publication at: https://www.researchgate.net/publication/229883251

Finely Dispersed Au Nanoparticles on SiO2 Achieved by the C-60 Additive and Their Catalytic Activity

ARTICLE *in* CHEMCATCHEM · JANUARY 2011

Impact Factor: 4.56 · DOI: 10.1002/cctc.201000342

CITATIONS
4

READS
27

5 AUTHORS, INCLUDING:

Kun Qian
University of Florida
28 PUBLICATIONS **806** CITATIONS
SEE PROFILE

Luo Liangfeng
University of Science and Technology of Ch…
8 PUBLICATIONS **61** CITATIONS
SEE PROFILE

Available from: Kun Qian
Retrieved on: 26 January 2016

DOI: 10.1002/cctc.201000342

Finely Dispersed Au Nanoparticles on SiO_2 Achieved by the C_{60} Additive and Their Catalytic Activity

Kun Qian,[a] Liangfeng Luo,[a] Chuanbao Chen,[b] Shangfeng Yang,[b] and Weixin Huang*[a]

We have investigated in detail the effect of buckminsterfullerene (C_{60}) additive on the structure and catalytic activity of Au/SiO_2 catalysts prepared by a routine deposition–precipitation method employing $HAuCl_4$ as the gold precursor. The structures of various catalysts have been characterized by using N_2 adsorption–desorption isotherms, powder X-ray diffraction, X-ray photoelectron spectroscopy, transmission electron microscopy, photoluminescence, and Raman spectroscopy. The C_{60} additive was found to greatly enhance the dispersion of Au nanoparticles supported on SiO_2. Supported Au nanoparticles that are about 3–5 nm in size can be synthesized without difficulty on C_{60}/SiO_2, whereas those sized about 7–10 nm are usually acquired on bare SiO_2. Strong Au–C_{60} interaction with the charge transfer from Au nanoparticles to C_{60} has been observed in Au/C_{60}/SiO_2 and proven to suppress the agglomeration of supported Au nanoparticles and enhance their dispersion on SiO_2. The catalyst Au/C_{60}/SiO_2-10 (Au:C_{60} molar ratio of 10) exhibits a much better catalytic performance for CO oxidation than Au/SiO_2, but is not active for CO oxidation at room temperature, which demonstrates that the intrinsic activity of supported Au nanoparticles increases with decreasing particle size, but supported Au 3–5 nm nanoparticles cannot activate oxygen for CO oxidation at room temperature. We propose that 3 nm is the critical size for Au nanoparticles to exhibit an intrinsic catalytic activity in CO oxidation at room temperature without additional contributions. These results provide novel and important insights into the fundamental understanding of intrinsic structure–activity relation of Au nanoparticles.

Introduction

Numerous supported Au catalysts active in low temperature CO oxidation have been synthesized by various methods[1] since Haruta et al. first reported that Au nanoparticles supported on TiO_2 and Fe_2O_3 could efficiently catalyze low-temperature CO oxidation.[2] It has been well established that the size and structure of supported Au nanoparticles have a determinative role in the catalytic activity of supported Au nanocatalysts in low temperature CO oxidation. The employed support greatly influences the size and structure of supported Au nanoparticles. By employing $HAuCl_4$ as the gold precursor, small Au nanoparticles, which are active in low temperature CO oxidation, can be synthesized on various transitional metal oxides (e.g., TiO_2, CeO_2, Fe_2O_3, Fe_3O_4, Co_3O_4, and ZnO) and Al_2O_3[1–9] by conventional incipient wetness impregnation (IWI) and deposition–precipitation (DP) methods; however, the related approaches have not been successful in preparing small and active Au nanoparticles supported on SiO_2.[10–14] This could be attributed to the weak interaction between the gold precursors and the SiO_2 surface during the course of catalyst preparation.

Although the Au/SiO_2 catalyst is not a good catalyst for low temperature CO oxidation, it is a good candidate for the fundamental investigation of structure–activity relation of supported Au catalysts. SiO_2 is an inert support and does not participate in the catalytic reaction so that the contribution of the support to the catalytic reaction can be minimized, therefore, the correlation between the geometric/electronic structures and the catalytic activity of supported Au nanoparticles can be unambiguously established in the Au/SiO_2 catalytic system.[15–18] The promotion effect of additives or other treatments on the catalytic activity is distinctly manifested for the Au/SiO_2 catalytic system because of its poor performance, which improves fundamental understanding.[11,14,19–24] Therefore, great effort has been devoted to the development of novel methods for the preparation of finely dispersed Au nanoparticles on SiO_2. Successful methods include chemical vapor deposition,[10] physical vapor deposition,[25] trapping Au nanoparticles in ordered mesoporous silica,[12,26] using micelle-derived Au nanoparticles[13] and cationic Au complexes ([Au(PPh_3)Cl], $[Au(en)_2]^{3+}$)[27–30] as gold precursors, and modifying SiO_2 by using active oxides.[20–23,31,32]

We report a novel method for the preparation of finely dispersed Au nanoparticles supported on SiO_2 acquired by the addition of buckminsterfullerene (C_{60}). C_{60} has attracted a lot of

[a] K. Qian,[+] L. Luo,[+] Prof. Dr. W. Huang
Hefei National Laboratory for Physical Sciences at the Microscale
CAS Key Laboratory of Materials for Energy Conversion
Department of Chemical Physics
University of Science and Technology of China
Jinzhai Road 96, Hefei 230026 (China)
Fax: (+86) 551-3600437
E-mail: huangwx@ustc.edu.cn

[b] C. Chen, Prof. Dr. S. Yang
Hefei National Laboratory for Physical Sciences at the Microscale
CAS Key Laboratory of Materials for Energy Conversion
Department of Materials Science and Engineering
University of Science and Technology of China
Jinzhai Road 96, Hefei 230026 (China)

[+] These authors contributed equally to this paper

 © 2011 Wiley-VCH Verlag GmbH & Co. KGaA, Weinheim

attention because of its unique structural and electronic features, but its applications in catalysis have seldom been explored. A non-metallic C_{60} molecule was reported to be capable of fixing nitrogen.[33] C_{60} and C_{70} were reported to be able to activate molecular hydrogen and thus be used as a nonmetal hydrogenation catalyst.[34] Metal–fullerene complexes have also been used as catalysts for catalytic hydrogenation[35] and a cooperation effect between C_{60} and C_{60}^-, formed by the metal–C_{60} electron transfer, was found to play important role.[36] Recently Xu et al.[37] prepared Ag/C_{60} catalysts and found that the Ag–C_{60} interaction plays an important role in the hydrogenation of aromatic nitro compounds. In our experiments, C_{60} was employed to modify the surface of SiO_2 and the acquired C_{60}/SiO_2 was further used for the preparation of $Au/C_{60}/SiO_2$ catalysts with a routine DP method by using $HAuCl_4$ as the gold precursor. Finely dispersed Au nanoparticles with a narrow size distribution of 3–6 nm were successfully prepared in $Au/C_{60}/SiO_2$ catalysts, smaller than those that dominate Au/SiO_2 catalysts. The Au–C_{60} interaction in $Au/C_{60}/SiO_2$ catalysts is suggested to account for the synthesis of finely dispersed Au nanoparticles. $Au/C_{60}/SiO_2$ catalysts show much better catalytic activity for CO oxidation than Au/SiO_2 catalysts, but are not active for CO oxidation at room temperature. These results imply that supported Au nanoparticles must be smaller than 3 nm to exhibit considerable intrinsic activity for low temperature CO oxidation without the involvement of oxide supports.

Results and Discussion

The catalytic performances of various catalysts in CO oxidation are shown in Figure 1. Au/SiO_2 exhibits a poor catalytic performance and becomes active at reaction temperatures above 210 °C, agreeing with our previous results.[14] The C_{60} additive clearly promotes the catalytic activity of supported Au nanoparticles for CO oxidation, as demonstrated by the much better catalytic performance of $Au/C_{60}/SiO_2$ than Au/SiO_2. The catalytic activity of $Au/C_{60}/SiO_2$ initially increases with the decrease of Au:C_{60} atomic ratio, and $Au/C_{60}/SiO_2$-10 exhibits the best catalytic activity with the T_{50} value (temperature for 50% CO conversion) being about 100 °C lower than that of Au/SiO_2. With further decreasing Au:C_{60} atomic ratio, the catalytic performance of Au/C_{60}/SiO2 decreases, which could be attributed to the covering of active Au sites by too much C_{60} additive. It is noteworthy that C_{60} in C_{60}/SiO_2 and $Au/C_{60}/SiO_2$ is thermally stable up to 330 °C in air, as evidenced by separate thermogravimetric analysis experiments and temperature programmed reaction spectroscopy (results not shown). Moreover, the CO conversion calculated from the change in CO concentrations in the inlet and outlet gases is the same as that calculated from the CO_2 concentration in the outlet gas measured by the chromatograph. These results demonstrate that the C_{60} in our catalysts is stable under the employed reaction conditions. We also prepared $C_{60}/Au/SiO_2$ to which C_{60} was added after the deposition of Au nanoparticles on SiO_2. It could be seen that the catalytic activity of $C_{60}/Au/SiO_2$ is worse than that of Au/SiO_2.

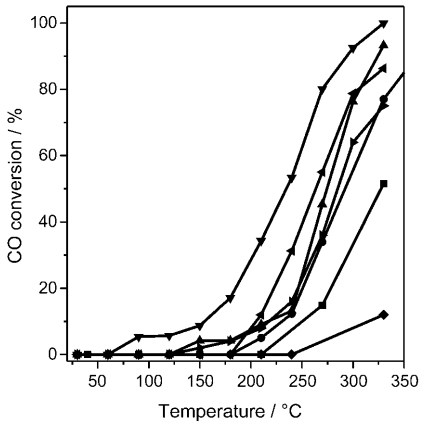

Figure 1. Catalytic performances of different catalysts in CO oxidation: Au/SiO_2 (■), $Au/C_{60}/SiO_2$-50 (●), $Au/C_{60}/SiO_2$-20 (▲), $Au/C_{60}/SiO_2$-10 (▼), $Au/C_{60}/SiO_2$-5 (◀),; $Au/C_{60}/SiO_2$-2 (▶), $C_{60}/Au/SiO_2$-10 (◆).

The Brunauer–Emmett–Teller (BET) surface area of Au/SiO_2 ($310\ m^2 g^{-1}$) and those of $Au/C_{60}/SiO_2$ catalysts did not vary much ($280–300\ m^2 g^{-1}$). Analysis of the inductively coupled plasma atomic emission spectroscopy (ICP-AES) results revealed the loaded gold content of all the catalysts (1.7–1.9%). The powder X-ray diffraction (XRD) patterns of all the catalysts (Figure 2) only displayed clearly visible diffraction peaks attributed to Au. Comparing those of Au/SiO_2, the diffraction peaks of $Au/C_{60}/SiO_2$ were broader, indicating that the average Au crystal nanoparticle size had decreased. On the basis of the Scherrer formula, the average Au crystal nanoparticle size was calculated from the full-width at half maximum (FWHM) of the Au(111) diffraction peak to be 12, 12, 7, 7, 7, 7, and 7 nm for $C_{60}/Au/SiO_2$-10, Au/SiO_2, $Au/C_{60}/SiO_2$-50, $Au/C_{60}/SiO_2$-20, $Au/C_{60}/SiO_2$-10, $Au/C_{60}/SiO_2$-5, and $Au/C_{60}/SiO_2$-2, respectively. Transmission electron microscopy (TEM) was employed to investigate the size distribution of the Au nanoparticles in Au/SiO_2 and $Au/C_{60}/SiO_2$-10 catalysts (Figure 3). Supported Au nanoparticles in Au/SiO_2 mostly exhibited a size distribution of 6–9 nm, in agreement with our previous results,[14] which was attributed to the weak interaction between the gold precursors and SiO_2

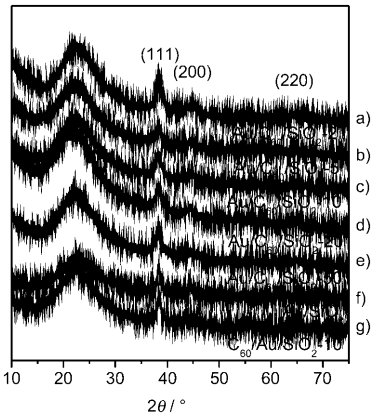

Figure 2. XRD patterns of different catalysts. a) $Au/C_{60}/SiO_2$-2, b) $Au/C_{60}/SiO_2$-5, c) $Au/C_{60}/SiO_2$-10, d) $Au/C_{60}/SiO_2$-20, e) $Au/C_{60}/SiO_2$-50, f) Au/SiO_2, g) $C_{60}/Au/SiO_2$-10.

 © 2011 Wiley-VCH Verlag GmbH & Co. KGaA, Weinheim

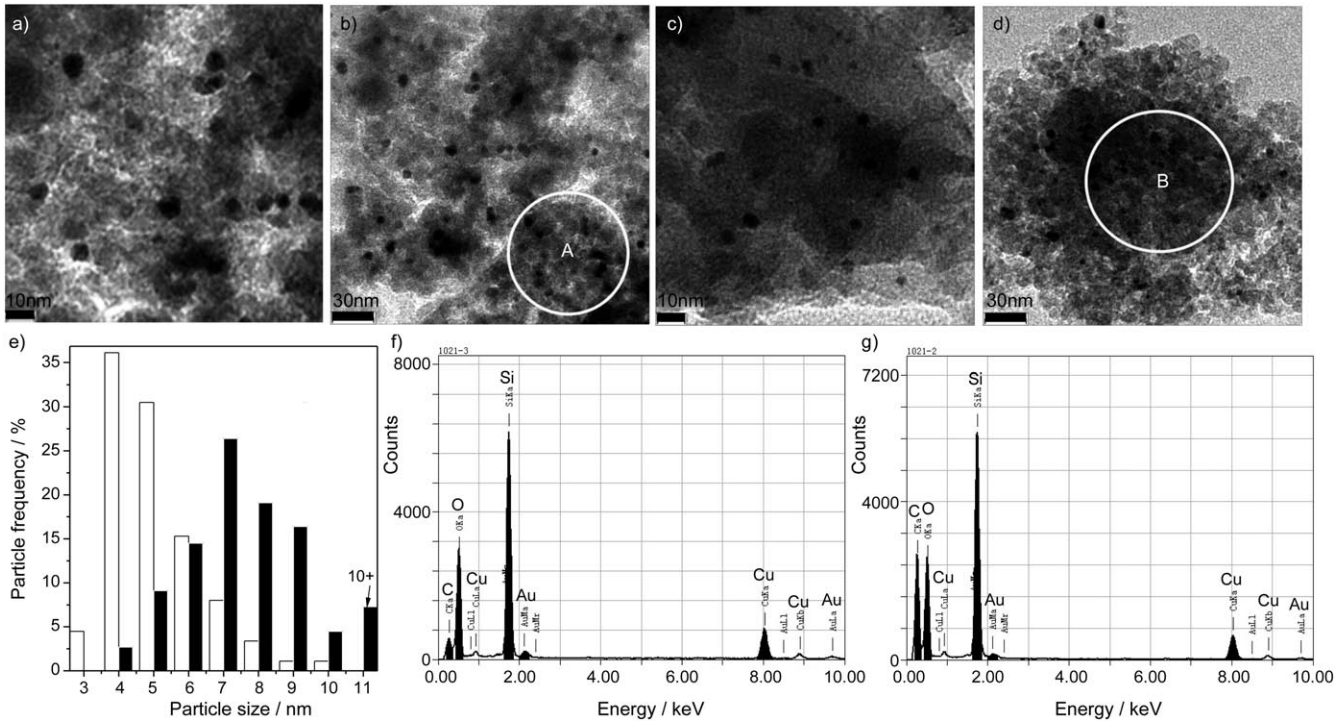

Figure 3. Representative TEM images of a,b) Au/SiO_2 and c,d) $Au/C_{60}/SiO_2$-10, the size distribution of supported Au nanoparticles in e) Au/SiO_2 (■) and $Au/C_{60}/SiO_2$-10 (□), and the EDX elemental analysis spectra of indicated areas A (f) and B (g).

surface during the course of the DP process. The Au nanoparticles in $Au/C_{60}/SiO_2$-10 were much smaller (3–7 nm). We counted the size of more than 100 Au nanoparticles for both catalysts, from which the size distribution of Au nanoparticles was plotted (Figure 1e). More than 70% of the Au nanoparticles were not larger than 5 nm in $Au/C_{60}/SiO_2$-10, whereas more than 70% Au nanoparticles were larger than 6 nm in Au/SiO_2. The average size of the Au nanoparticles was calculated from TEM results to be 8.9 nm for Au/SiO_2 and 5.4 nm for $Au/C_{60}/SiO_2$-10. The C_{60} additive clearly exhibited a promotion effect for the dispersion of Au nanoparticles supported on inert SiO_2. Further analysis of the elemental compositions of areas A and B of Figure 1b,d by using energy dispersive X-ray spectrometry (EDS) (Figure 1f). Although C_{60} in the catalyst could not be directly imaged by TEM, area B in $Au/C_{60}/SiO_2$-10 with small Au nanoparticles showed a much higher carbon content than that in the area A in Au/SiO_2, which had large Au nanoparticles (Figure 1f,g), indicating that small Au nanoparticles are located together with C_{60} in $Au/C_{60}/SiO_2$-10.

The photoluminescence (PL) spectra shown in Figure 4 also provides evidence that small Au nanoparticles are located together with C_{60} in $Au/C_{60}/SiO_2$-10. Excited by the $\lambda = 320$ nm laser, SiO_2 exhibits a strong, broad, and asymmetric fluorescence band centered at $\lambda = 400$ nm. The loading of Au nanoparticles greatly quenched the fluorescence of SiO_2, supporting the existence of an Au–SiO_2 interaction, which, in turn, results in the non-irradiative relaxation of excitons formed in SiO_2. The quenching effect of C_{60} on the fluorescence of SiO_2 was more pronounced than that for Au nanoparticles. However, we found that the fluorescence spectrum of $Au/C_{60}/SiO_2$-10 was similar to that of C_{60}/SiO_2-10, therefore the loading of Au nanoparticles on C_{60}/SiO_2-10 did not result in additional quenching channels for the fluorescence of SiO_2. As the Au nanoparticles supported on SiO_2 also effectively quench the fluorescence of SiO_2, this observation indicates that the Au nanoparticles in $Au/C_{60}/SiO_2$ mostly interact with C_{60}. Therefore, a strong interaction exists between Au nanoparticles and C_{60} in the $Au/C_{60}/SiO_2$ catalysts, which we believe act to stabilize the small Au nanoparticles.

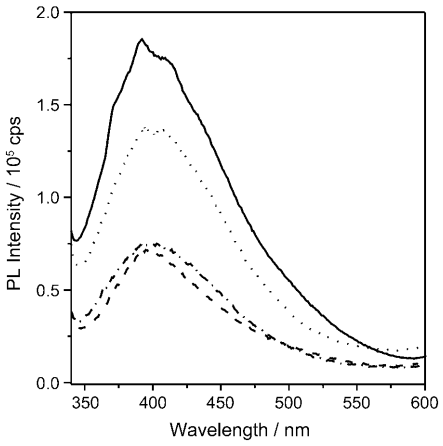

Figure 4. Photoluminescence spectra of different catalysts: SiO_2-5 (——), C_{60}/SiO_2-10 (-----), $Au/C_{60}/SiO_2$-10 (–•–•), Au/SiO_2 (••••).

The C_{60} additive has been demonstrated to effectively enhance the dispersion of Au nanoparticles supported on SiO_2 through strong Au–C_{60} interaction. Raman spectroscopy is a sensitive technique to probe C_{60} and was employed to get further insight into the nature of the Au–C_{60} interaction in $Au/C_{60}/$

 © 2011 Wiley-VCH Verlag GmbH & Co. KGaA, Weinheim

SiO_2 catalysts. The Raman spectra of C_{60}/SiO_2-5, C_{60}/SiO_2-10, Au/C_{60}/SiO_2-5, and Au/C_{60}/SiO_2-10 is shown in Figure 5. Five bands were observed at $\tilde{\nu}=269$, 496, 1424, 1468, 1569 cm^{-1} for C_{60}/SiO_2-5 and C_{60}/SiO_2-10, which were assigned to $H_g(1)$, $A_g(1)$, $H_g(7)$, $A_g(2)$, and $H_g(8)$ vibrational modes of C_{60} supported on SiO_2, respectively, in reference to the Raman spectra of pure C_{60}.[39,40] The Raman vibrational bands of C_{60} greatly weaken after the loading of Au nanoparticles. The $H_g(7)$ vibrational mode at $\tilde{\nu}=1424$ cm^{-1} disappear for Au/C_{60}/SiO_2-5 and only $A_g(2)$, and $H_g(8)$ vibrational modes could be well resolved for Au/C_{60}/SiO_2-10. The $H_g(8)$ vibrational mode broadens and shifts from $\tilde{\nu}=1569$ cm^{-1} for C_{60}/SiO_2 to $\tilde{\nu}=1578$ cm^{-1} for Au/C_{60}/SiO_2. The $A_g(2)$ vibrational mode slightly broadens and shifts from $\tilde{\nu}=1468$ cm^{-1} for C_{60}/SiO_2 to $\tilde{\nu}=1465$ cm^{-1} for Au/C_{60}/SiO_2. The downshift of the $A_g(2)$ vibrational mode of C_{60} in metal–C_{60} composites has been proposed to be an indication of the existence of charge transfer from metal to C_{60}.[39–41] Therefore, the Raman spectra results further confirmed the existence of a strong Au–C_{60} interaction by means of the charge transfer from Au nanoparticles to C_{60} in Au/C_{60}/SiO_2 catalysts. However, the charge transfer in Au/C_{60}/SiO_2 catalysts was much less pronounced than for previously reported metal–C_{60} nanostructured films in which the $A_g(2)$ vibrational mode shifts downwards by about 8–10 cm^{-1}.[40]

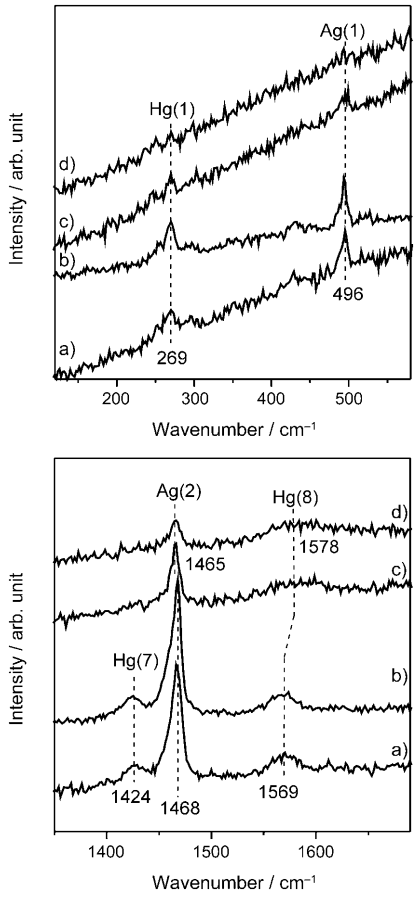

Figure 5. Raman spectra of a) C_{60}/SiO_2-5, b) C_{60}/SiO_2-10, c) Au/C_{60}/SiO_2-5, and d) Au/C_{60}/SiO_2-10.

We also investigated the calcination process of the precursor of Au/C_{60}/SiO_2-10 by means of Raman spectroscopy (Figure 6). The gold species in the precursor of the Au/C_{60}/SiO_2 catalysts dried at 60 °C mainly consists of $[Au(OH)_3Cl]^-$ and $[Au(OH)_4]^-$.[42] Although with reduced intensities, five Raman vibrational bands with the same position as those in C_{60}/SiO_2-10 were visible in the Raman spectra of Au/C_{60}/SiO_2-10 precursor, which indicated that the gold species do not interact strongly with C_{60} in the Au/C_{60}/SiO_2-10 precursor. The Raman spectrum changed greatly after the Au/C_{60}/SiO_2-10 precursor was calcined at 120 °C, at which temperature metallic Au nuclei begin to appear in the sample. Therefore, these results suggest that the strong interaction occurs first, between C_{60} and the metallic Au nuclei, in the sample that subsequently suppresses the growth of Au nanoparticles and eventually enhances the dispersion of Au nanoparticles on SiO_2.

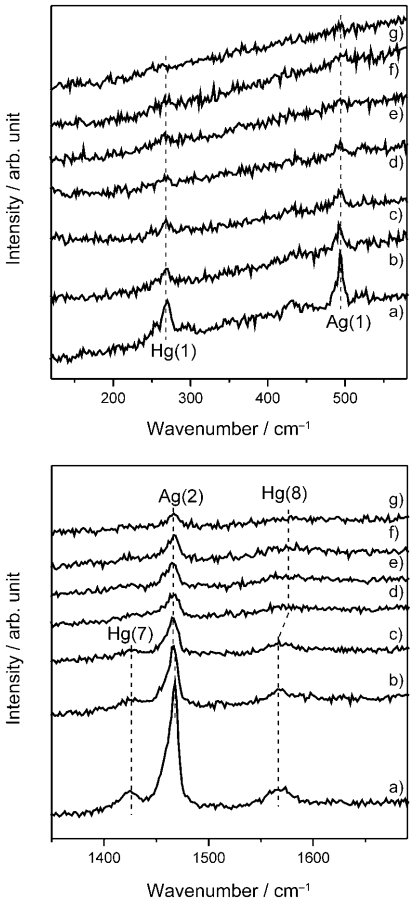

Figure 6. Raman spectra of a) C_{60}/SiO_2-10, the precursor of b) Au/C_{60}/SiO_2-10, and the precursor of Au/C_{60}/SiO_2-10 calcined at c) 90, d) 120, e) 150, f) 180 and g) 200 °C.

The Au 4f XPS spectra of various catalysts are presented in Figure 7. The Au 4f XPS spectra of Au/SiO_2 and Au/C_{60}/SiO_2 are similar, consisting of a single component. The Au $4f_{7/2}$ binding energy is located at 83.8 eV for Au/SiO_2 and slightly shifts upward to 84.0 eV for Au/C_{60}/SiO_2 with the decrease of the Au:C_{60} atomic ratio. Both values are characteristic for metallic Au and the slightly higher Au $4f_{7/2}$ binding energy of Au nano-

 © 2011 Wiley-VCH Verlag GmbH & Co. KGaA, Weinheim

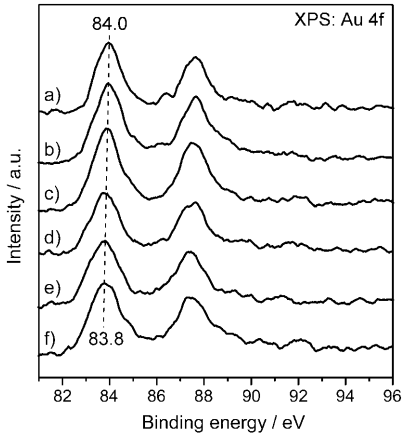

Figure 7. Au 4f XPS spectra of different catalysts. a) $Au/C_{60}/SiO_2$-2; b) $Au/C_{60}/SiO_2$-5; c) $Au/C_{60}/SiO_2$-10; d) $Au/C_{60}/SiO_2$-20; e) $Au/C_{60}/SiO_2$-50; f) Au/SiO_2.

particles in $Au/C_{60}/SiO_2$ than that in Au/SiO_2 indicates that the Au nanoparticles in $Au/C_{60}/SiO_2$ are slightly positively charged. This is in agreement with the Raman spectra results that the charge transfer exists from Au nanoparticles to C_{60} in $Au/C_{60}/SiO_2$. It has been reported that the positively charged Au species plays an important role in catalyzing low temperature CO oxidation.[43]

Our results provide a novel and convenient method to synthesize highly-dispersed Au nanoparticles supported on SiO_2 by DP employing $HAuCl_4$ as the gold precursor. Supported Au nanoparticles (3–5 nm) can be simply synthesized on C_{60}/SiO_2, whereas the larger sizes (7–10 nm) are usually acquired on bare SiO_2. Strong Au–C_{60} interaction with the charge transfer from Au nanoparticles to C_{60} has been observed in $Au/C_{60}/SiO_2$ and proven to suppress the agglomeration of supported Au nanoparticles and thus enhance their dispersion on SiO_2. Comparing previously reported methods for the preparation of small Au nanoparticles on SiO_2,[10,12,13,20–32] our method has the following advantages: first, our method is very convenient. DP is one of the most routine methods for the synthesis of supported catalysts and $HAuCl_4$ is the most common gold compound. Previous methods, such as chemical vapor deposition,[10] physical vapor deposition,[25] trapping Au nanoparticles in ordered mesoporous silica,[12,26] using micelle-derived Au nanoparticles,[13] and cationic Au complex ($Au(PPh_3)Cl$, $[Au(en)_2]^{3+}$)[27–30] as gold precursors, involve either a complicate apparatus or uncommon gold compounds; second, C_{60} and SiO_2 in $Au/C_{60}/SiO_2$ catalysts do not participate the catalytic reaction and thus the intrinsic structure–activity relation of supported Au nanoparticles can be derived. Previous methods such as modifying SiO_2 by the active oxides[20–23,31,32] are not able to exclude the contribution of active oxides to the catalytic activity of catalysts in CO oxidation. $Au/C_{60}/SiO_2$-10 exhibits much better catalytic performance in CO oxidation than Au/SiO_2, but is not active for CO oxidation catalysis at room temperature. This clearly demonstrates that the intrinsic activity of supported Au nanoparticles increases with decreasing particle size, but the smaller supported Au nanoparticles (3–5 nm) still cannot activate oxygen for CO oxidation at room temperature. Namely, the active oxide support should be involved in CO oxidation at room temperature catalyzed by small supported Au nanoparticles (3–5 nm). Recently Gajan et al. reported that smaller Au nanoparticles (1.8–4.0 nm) supported on SiO_2 can catalyze CO oxidation at the room temperature.[44] Therefore, 3 nm seems to be a critical size for Au nanoparticles to exhibit an intrinsic catalytic activity in CO oxidation at room temperature without contributions from elsewhere.

Conclusions

We have successfully developed a novel method for the synthesis of small Au nanoparticles supported on SiO_2 by the addition of C_{60} employing a DP method and $HAuCl_4$ as the gold precursor. Supported Au nanoparticles (3–5 nm) sizes can be simply synthesized on C_{60}/SiO_2, whereas the larger nanoparticles (7–10 nm) are usually acquired on bare SiO_2. Strong Au–C_{60} interaction with the charge transfer from Au nanoparticles to C_{60} in $Au/C_{60}/SiO_2$ has been proven to suppress the agglomeration of supported Au nanoparticles and thus enhance their dispersion on SiO_2. $Au/C_{60}/SiO_2$-10 exhibits much better catalytic performance in CO oxidation than Au/SiO_2, but is not active for CO oxidation catalysis at room temperature, which demonstrates that the intrinsic activity of supported Au nanoparticles increases with the decreasing particle size. Supported 3–5 nm Au nanoparticles still cannot activate oxygen for CO oxidation at room temperature. Therefore, we proposed that 3 nm is a critical size for Au nanoparticles to exhibit an intrinsic catalytic activity in CO oxidation at room temperature without contributions from elsewhere. These results provide novel and important insights into the fundamental understanding of the structure–activity relationship of Au nanoparticles.

Experimental Section

Buckminsterfullerene (C_{60}) was synthesized by the Krätschmer–Huffman DC-arc discharging method and isolated by high performance liquid chromatography (HPLC).[38] SiO_2 (40–120 mesh, Qingdao Haiyang Chemicals Co.) was first modified with saturated C_{60} solution in toluene (3.9×10^{-3} M) by using the IWI method followed by drying at 60 °C overnight and calcination at 200 °C in air for 4 h. The same IWI step was repeated to prepare C_{60}/SiO_2 catalysts with higher C_{60} loadings. The resultant C_{60}/SiO_2 catalysts were then used to prepare $Au/C_{60}/SiO_2$ catalysts by using the DP method with $HAuCl_4{\cdot}4H_2O$ (Sinopharm Chemical Reagent Co., Ltd, Au content $\geq$47.8%) as the precursor. In our experiments, the calculated loading of Au in all $Au/C_{60}/SiO_2$ catalysts was kept at 2% (Au:SiO_2 weight ratio). Typically, $HAuCl_4{\cdot}4H_2O$ (0.9663 g) was dissolved in distilled water (50 mL) to prepare an $HAuCl_4$ aqueous solution (0.0469 mol L^{-1}) . $HAuCl_4$ aqueous solution (4.33 mL), C_{60}/SiO_2 (2.0 g) with the desired C_{60} loadings, and distilled water (45.7 mL) were added into a three-neck bottle stirred at 60 °C for 30 min. An appropriate amount of ammonium hydroxide was added to adjust the pH value of the solution to 9–10, and then the mixture was stirred at 60 °C for 24 h. The solid was then filtered, washed with distilled water several times, dried at 60 °C for 24 h, and finally calcined at 200 °C in air for 4 h. The $Au/C_{60}/SiO_2$ catalyst with a Au:C_{60} molar ratio of x was denoted as $Au/C_{60}/SiO_2$-x.

The $C_{60}/Au/SiO_2$ catalysts were prepared by using a similar method but with a reverse loading order of C_{60} and Au for comparison. The

 © 2011 Wiley-VCH Verlag GmbH & Co. KGaA, Weinheim

2%-Au/SiO_2 catalyst was prepared by using the DP method followed by calcination at 200 °C in air for 4 h. The product was used as the precursor for loading the C_{60} additive by the IWI method followed by calcination at 200 °C in air for 4 h.

The composition of catalysts was analyzed by using inductively coupled plasma atomic emission spectrometry (ICP-AES). BET surface areas were acquired by using a Beckman Coulter SA3100 surface area analyzer, in which the sample was degassed at 120 °C for 30 min in a nitrogen atmosphere before the measurements. Powder X-ray diffraction (XRD) spectra were acquired by using a Philips X'Pert PRO SUPER X-ray diffractometer with a Ni-filtered $Cu_{K\alpha}$ X-ray source operating at 40 kV and 50 mA. X-ray photoelectron spectroscopy (XPS) measurements were performed by using an ESCALAB 250 electron spectrometer with a monochromatized $Al_{K\alpha}$ excitation source ($h\nu = 1486.6$ eV). The binding energies of the XPS spectra were referenced with respect to the Si 2p binding energy in SiO_2 at 103.3 eV. Transmission electron microscopy (TEM) was performed by using a JEOL 2010 transmission electron microscope. Photoluminescence (PL) spectra were acquired by using a Fluorolog-Tau-3 steady-state/lifetime spectrofluorometer. Raman spectra were acquired by using the back-scattering configuration on a LABRAM-HR Confocal Laser Raman Spectrometer using the visible Ar^+ laser ($\lambda = 514.5$ nm) as the excitation source and the time of acquisition was 60 s.

The catalytic activity was evaluated with a fixed-bed flow reactor. The catalyst experienced no pretreatment prior to the catalytic reaction. The used catalyst weight was 100 mg and the reaction gas consisted of 1% CO and 99% dry air and was fed at a rate of 20 mL min^{-1}. The composition of the effluent gas was detected by using an online GC-14C gas chromatograph equipped with a TDX-01 column ($T = 80$ °C, H_2 as the carrier gas at 30 mL min^{-1}). The conversion of CO was calculated both from the change in CO concentrations in the inlet and outlet gases and from the CO_2 concentration in the outlet gas.

Acknowledgements

This work was financially supported by National Natural Science Foundation of China (grants 20801052, 20973161), the Ministry of Science and Technology of China (2010CB923302), the MOE program for PCSIRT (IRT0756), the Fundamental Research Funds for the Central Universities (WK2060030005), and the MPG-CAS partner group program.

Keywords: dispersion · fullerenes · gold · oxidation · structure–activity relationships

[1] M. Haruta, *CATTECH* **2002**, *6*, 102 – 115.
[2] M. Haruta, M. Yamada, T. Kobayashi, S. Iijima, *J. Catal.* **1989**, *115*, 301 – 309.
[3] M. M. Schubert, S. Hackenberg, A. C. van Veen, M. Muhler, V. Plzak, R. J. Behm, *J. Catal.* **2001**, *197*, 113 – 122.
[4] K. R. Souza, A. F. F. de Lima, F. F. de Sousa, L. G. Appel, *Appl. Catal. A* **2008**, *340*, 133 – 139.
[5] J.-Y. Yan, M. C. Kung, W. M. H. Sachtler, H. H. Kung, *J. Catal.* **1997**, *172*, 178 – 186.
[6] F. Moreau, G. C. Bond, A. O. Taylor, *J. Catal.* **2005**, *231*, 105 – 114.
[7] D. Widmann, R. Leppelt, R. J. Behm, *J. Catal.* **2007**, *251*, 437 – 442.
[8] M. Khoudiakov, M. C. Gupta, S. Deevi, *Appl. Catal. A* **2005**, *291*, 151 – 161.
[9] M. Á. Centeno, C. Portales, I. Carrizosa, J. A. Odriozola, *Catal. Lett.* **2005**, *102*, 289 – 297.
[10] M. Okumura, S. Nakamura, S. Tsubota, T. Nakamura, M. Azuma, M. Haruta, *Catal. Lett.* **1998**, *51*, 53 – 58.
[11] M. A. P. Dekkers, M. J. Lippits, B. E. Nieuwenhuys, *Catal. Today* **1999**, *54*, 381 – 390.
[12] S. H. Overbury, L. Ortiz-Soto, H. Zhu, B. Lee, M. D. Amiridis, S. Dai, *Catal. Lett.* **2004**, *95*, 99 – 106.
[13] J. Chou, N. R. Franklin, S. H. Baeck, T. F. Jaramillo, E. W. McFarland, *Catal. Lett.* **2004**, *95*, 107 – 111.
[14] K. Qian, Z. Jiang, W. Huang, *J. Mol. Catal. A* **2007**, *264*, 26 – 32.
[15] L. Guczi, G. Peto, A. Beck, K. Frey, O. Geszti, G. Molnár, C. Daróczi, *J. Am. Chem. Soc.* **2003**, *125*, 4332 – 4337.
[16] D. C. Lim, I. Lopez-Salido, R. Dietsche, M. Bubek, Y. D. Kim, *Angew. Chem.* **2006**, *118*, 2473 – 2475; *Angew. Chem. Int. Ed.* **2006**, *45*, 2413 – 2415.
[17] N. Weiher, E. Bus, L. Delannoy, C. Louis, D. E. Ramaker, J. T. Miller, J. A. van Bokhoven, *J. Catal.* **2006**, *240*, 100 – 107.
[18] J. T. Miller, A. J. Kropf, Y. Zha, J. R. Regalbuto, L. Delannoy, C. Louis, E. Bus, J. A. van Bokhoven, *J. Catal.* **2006**, *240*, 222 – 234.
[19] L. Guczi, D. Horváth, Z. Pászti, L. Tóth, Z. E. Horváth, A. Karacs, G. Petõ, *J. Phys. Chem. B* **2000**, *104*, 3183 – 3193.
[20] K. Qian, W. X. Huang, Z. Q. Jiang, H. X. Sun, *J. Catal.* **2007**, *248*, 137 – 141.
[21] K. Qian, W. X. Huang, J. Fang, S. S. Lv, B. He, Z. Q. Jiang, S. Q. Wei, *J. Catal.* **2008**, *255*, 269 – 278.
[22] K. Qian, J. Fang, W. Huang, B. He, Z. Jiang, Y. Ma, S. Wei, *J. Mol. Catal. A* **2010**, *320*, 97 – 105.
[23] K. Qian, S. Lv, X. Xiao, H. Sun, J. Lu, M. Luo, W. Huang, *J. Mol. Catal. A* **2009**, *306*, 40 – 47.
[24] K. Qian, H. X. Sun, W. X. Huang, J. Fang, S. S. Lv, B. He, Z. Q. Jiang, S. Q. Wei, *Chem. Eur. J.* **2008**, *14*, 10595 – 10602.
[25] G. M. Veith, A. R. Lupini, S. Rashkeev, S. J. Pennycook, D. R. Mullins, V. Schwartz, C. A. Bridges, N. J. Dudney, *J. Catal.* **2009**, *262*, 92 – 101.
[26] H. G. Zhu, B. Lee, S. Dai, S. H. Overbury, *Langmuir* **2003**, *19*, 3974 – 3980.
[27] G. Martra, L. Prati, C. Manfredotti, S. Biella, M. Rossi, S. Coluccia, *J. Phys. Chem. B* **2003**, *107*, 5453 – 5459.
[28] R. Zanella, A. Sandoval, P. Santiago, V. A. Basiuk, J. M. Saniger, *J. Phys. Chem. B* **2006**, *110*, 8559 – 8565.
[29] H. G. Zhu, C. D. Liang, W. F. Yan, S. H. Overbury, S. Dai, *J. Phys. Chem. B* **2006**, *110*, 10842 – 10848.
[30] H. G. Zhu, Z. Ma, J. C. Clark, Z. W. Pan, S. H. Overbury, S. Dai, *Appl. Catal. A* **2007**, *326*, 89 – 99.
[31] L. Guczi, K. Frey, A. Beck, G. Petõ, C. S. Daróczi, N. Kruse, S. Chenakin, *Appl. Catal. A* **2005**, *291*, 116 – 125.
[32] C. L. Peza-Ledesma, L. Escamilla-Perea, R. Nava, B. Pawelec, J. L. G. Fierro, *Appl. Catal. A* **2010**, *375*, 37 – 48.
[33] Y. Nishibayashi, M. Saito, S. Uemura, S. Takekuma, H. Takekuma, Z. Yoshida, *Nature* **2004**, *428*, 279 – 280.
[34] B. J. Li, Z. Xu, *J. Am. Chem. Soc.* **2009**, *131*, 16380 – 16382.
[35] E. Sulman, Y. Bodrova, V. Matveeva, N. Semagina, L. Cerveny, V. Kurtc, L. Bronstein, O. Platonova, P. Valetsky, *Appl. Catal. A* **1999**, *176*, 75 – 81.
[36] G. Accorsi, N. Armaroli, *J. Phys. Chem. C* **2010**, *114*, 1385 – 1403.
[37] B. J. Li, H. B. Li, Z. Xu, *J. Phys. Chem. C* **2009**, *113*, 21526 – 21530.
[38] L. Dunsch, S. Yang, *Small* **2007**, *3*, 1298 – 1320.
[39] D. S. Bethune, G. Meijier, W. C. Tang, H. J. Rosen, W. G. Golden, H. Seki, C. A. Brown, M. S. de Vries, *Chem. Phys. Lett.* **1991**, *179*, 181 – 186.
[40] M. G. Mitch, S. J. Chase, J. S. Lannin, *Phys. Rev. Lett.* **1992**, *68*, 883 – 886.
[41] W. I. F. David, R. M. Ibberson, J. C. Matthewman, K. Prassides, T. Dennis, J. P. Hare, H. W. Kroto, R. Taylor, D. Walton, *Nature* **1991**, *353*, 147 – 149.
[42] S. Wang, K. Qian, X. Z. Bi, W. X. Huang, *J. Phys. Chem. C* **2009**, *113*, 6505 – 6510.
[43] M. C. Kung, R. J. Davis, H. H. Kung, *J. Phys. Chem. C* **2007**, *111*, 11767 – 11775.
[44] D. Gajan, K. Guillois, P. Delichere, J. M. Basset, J. P. Candy, V. Caps, C. Coperet, A. Lesage, L. Emsley, *J Am Chem. Soc.* **2009**, *131*, 14667 – 14669.

Received: September 24, 2010
Published online on December 14, 2010

 © 2011 Wiley-VCH Verlag GmbH & Co. KGaA, Weinheim